Exp. Theo. NANOTECHNOLOGY 10 (2026) 229-237 https://doi.org/10.56053/10.S.229

Effect of TiO_2 on structural and morphological properties of PMMA/TiO_2 nanostructures prepared by dip coating: different concentration from TiO_2

Hussein A. Hammood[*], *Ghada A. Kadhim*

Department of physics College of Science, University of Wasit, Wasit, Iraq
[*]) Email: std.2023hhammoud@uowasit.edu.iq

Received 17/11/2025, *Received in revised form* 15/12/2025, *Accepted* 28/12/2025, *Published* 15/2/2026

Nanocomposite thin films of (PMMA/TiO_2) are deposited onto glass substrates using the dip-coating technique. The films are prepared from pure PMMA and (PMMA/TiO_2) composites with different molar concentrations of TiO_2. XRD, FE-SEM, FTIR, and AFM analyses are employed to investigate the structural and morphological properties of the thin films. XRD results revealed that the pure PMMA film exhibited an amorphous structure, while the (PMMA/TiO_2) composites showed additional crystalline peaks around 30° corresponding to the (101) orientation. FE-SEM images demonstrated a transition in surface morphology—from a smooth and homogeneous texture for pure PMMA to more pronounced crystalline branched structures with increasing TiO_2 content. FTIR spectra confirmed the characteristic peaks of both pure PMMA and (PMMA/TiO_2) films. Upon TiO_2 incorporation, a new Ti–O vibration peak appeared at 800 cm^{-1}. AFM topographic analysis quantified these changes, showing an increase in the average grain diameter from 18.58 nm (pure PMMA) to 21.65 nm (PMMA/0.3 M TiO_2), while the surface roughness decreased from 168.0 pm to 158.1 pm. The peak-to-peak distance also decreased from 983.7 pm to 721.0 pm, indicating enhanced surface uniformity. These results confirm that the obtained thin films possess good structural and surface properties, qualifying them for use in various applications.

Keywords: Nanostructure; PMMA; TiO_2.

1. INTRODUCTION

A composite is defined as any physical combination of two or more different materials that produces a new material with properties that cannot be achieved by each component individually [1,2]. The properties of composites can be improved by adding inorganic molecules [3]. Nanocomposites enhance the usability of biodegradable polymers by increasing their thermal stability. Polymer nanocomposites are defined as polymers that contain nanoscale fillers, and their microstructure exhibits inhomogeneous regions within the nanometre range [4].

A wide range of polymers are commonly used for various applications. Among these, polymethyl methacrylate (PMMA) is a synthetic polymer prepared by free-radical addition and polymerization of methyl methacrylate ($C_5O_2H_8$) to form poly(methyl methacrylate) $(C_5O_2H_8)_n$ [5]. Acrylic, which is often used as a glass substitute, can also be utilized in various applications due to its versatile properties [6].

Many studies have investigated the effect of reinforcement with titanium dioxide (TiO_2) particles to improve PMMA characteristics such as hardness, fracture toughness, and flexural strength [7]. Titanium dioxide (titania, TiO_2) is a chemically inert, semiconducting material that also exhibits photocatalytic activity in the presence of light with energy equal to or higher than its band-gap energy. These characteristics provide a wide range of potential applications. Moreover, due to the relatively low cost of the raw material and its ease of processing, titania has gained widespread attention over recent decades [8].

Information sensing is essentially an energy transfer process in which energy is transmitted from the measured object to the sensor, making all sensors act as energy converters [9]. Humidity sensors, in particular, have gained increasing importance in industrial processing and environmental control applications [10]. Dip coating represents one of the oldest commercially applied coating processes. In the standard approach, the substrate is withdrawn vertically from the solution reservoir at a constant speed (U_0) [11]. The aim of this work is to prepare pure thin films of PMMA and nanocomposite films of (PMMA/TiO_2), and to study their structural and morphological properties.

2. EXPERIMENTAL

2.1 Materials

Liquid PMMA (Chinese origin, 100% purity) and titanium dioxide (TiO_2, Chinese origin, 99.9% purity) are used in this study.

2.2 *Method*

The solution used for depositing the thin films is prepared from pure PMMA by adding 40 mL of liquid PMMA into a beaker. For the preparation of the nanocomposite thin films (PMMA/TiO_2), different concentrations of TiO_2 (0.1, 0.2, and 0.3 M) are obtained by adding corresponding weights of 0.3196, 0.6392, and 0.9588 g, respectively, to 40 mL of liquid PMMA. The amount of TiO_2 added is calculated using the following equation:

$$M = \frac{wt}{Mw} X \frac{1000}{V(ml)} \quad (1)$$

where M is the molarity (mol L^{-1}), wt is the weight in grams (g), M_w is the molecular weight in g mol^{-1}, and V is the volume in millilitres (mL). The molecular weight of TiO_2 is 79.9 g mol^{-1}.

The prepared solution is placed in a beaker inside a water bath maintained at 60 °C, with continuous stirring until a homogeneous mixture is obtained. The beaker is then removed, and each thin-film sample is dip-coated four times, with each immersion lasting 4 s. The coated samples are subsequently left to dry at room temperature.

The structural properties of the samples are characterized using an X-ray diffractometer (Aeris Research Edition) equipped with a Cu target. The microstructure of the films is examined using a Hitachi FE-SEM (Model S4160). Fourier-transform infrared spectroscopy (FTIR) analysis is carried out using an ALPHA II spectrometer (IEC/EN 60825-1:2014, Germany). The topographic properties of the films are investigated by atomic-force microscopy (AFM) using an AA3000 Scanning Probe Microscope.

3. RESULTS AND DISCUSSION

3.1 X-ray diffraction analysis (XRD)

The structural properties of the prepared thin films are analyzed using X-ray diffraction (XRD) patterns, as shown in Figure 1. For pure PMMA, an amorphous pattern is observed with a broad halo located within the diffraction angles of (10–23) °, which agrees with previous findings [1]. Upon the gradual addition of TiO_2 and the formation of (PMMA/TiO_2) nanocomposite thin films, a distinct crystallization peak appeared at approximately 30°, corresponding to the (101) orientation.

Both the intensity and crystallite size are found to increase, as calculated using Scherrer's equation [12]:

$$D = \frac{k\lambda}{\beta cos\theta} \quad (2)$$

where D is the crystallite size, λ is the X-ray wavelength (1.54060 Å), β is the full width at half maximum (FWHM) of the diffraction peak, θ is the Bragg angle, and k is a constant (0.9).

The FWHM of the peaks decreases as TiO_2 content increases, accompanied by a reduction in the amorphous halo intensity. This behavior indicates the appearance of crystalline regions induced by TiO_2 incorporation, since TiO_2 is a crystalline oxide. As its concentration increases, the number of oriented crystallites in the (101) direction also rises. Table 1 lists the main structural parameters determined from the XRD analysis.

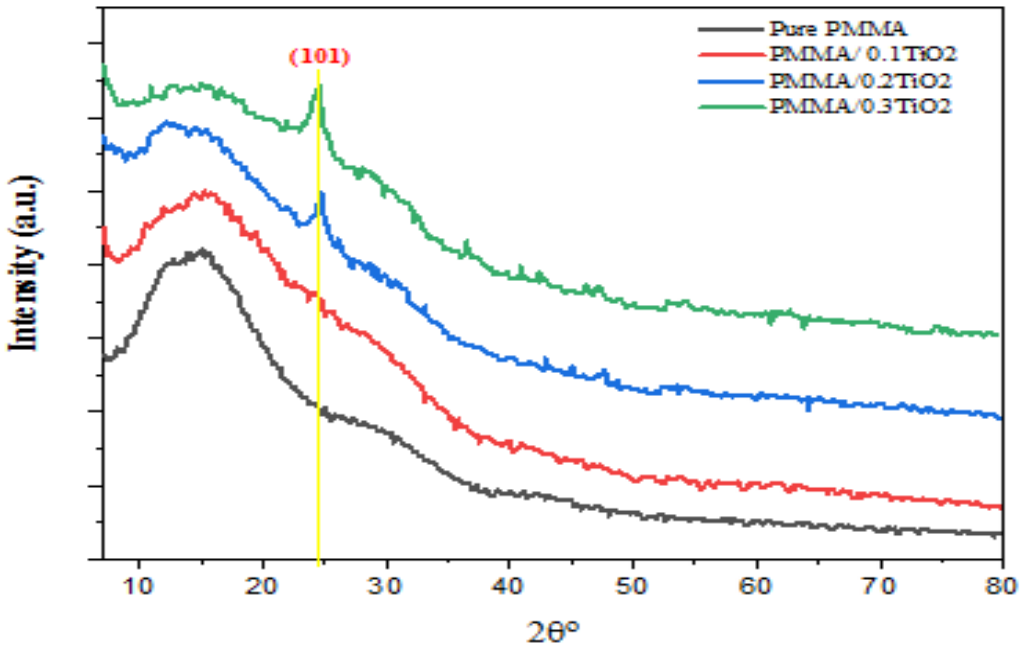

Figure 1 XRD patterns of pure PMMA and (PMMA/TiO_2) nanocomposite thin films prepared with different TiO_2 concentrations via dip coating at 60 °C.

Table 1 XRD parameters and crystallographic data for pure PMMA and (PMMA/TiO_2) nanocomposites with varying TiO_2 content.

Samples	2θ (degrees)	Miller Indices (hkl)	d-spacing [Å]	FWHM	Crystallite Size [Å]	Notes
PMMA	10º-23º	-	-	-	-	Broad peak (amorphous region)
PMMA/0.1TiO₂	10º-23º	-	-	-	-	Broad peak (amorphous region)
	25.3°	(101)	-	-	-	Weak peak Main anatase peak
PMMA/0.2TiO₂	10º-23º	-	-	-	-	Broad peak (amorphous region)
	24.343°	(101)	3.6535	3.2116	14	-
PMMA/0.3TiO₂	10º-23º	-	-	-	-	Broad peak (amorphous region)
	24.5878°	(101)	3.61767	2.9655	15	-

3.2 Field emission-scanning electron microscopy (FE-SEM)

The surface morphology of pure PMMA and (PMMA/TiO_2) thin films with various TiO_2 ratios (0.1, 0.2, and 0.3 M) prepared at 60 °C is examined using field emission scanning electron microscopy (FE-SEM), as presented in Figure 2. The micrographs show that the pure PMMA thin film exhibits a smooth and homogeneous surface free from agglomerations, as shown in Figure 2a. When TiO_2 is incorporated, branched crystalline structures emerge and intertwine with the polymer matrix, leading to a rougher and more textured surface. With higher TiO_2 content, the degree of agglomeration becomes more pronounced, as clearly observed in Figures (2 b,c,d).

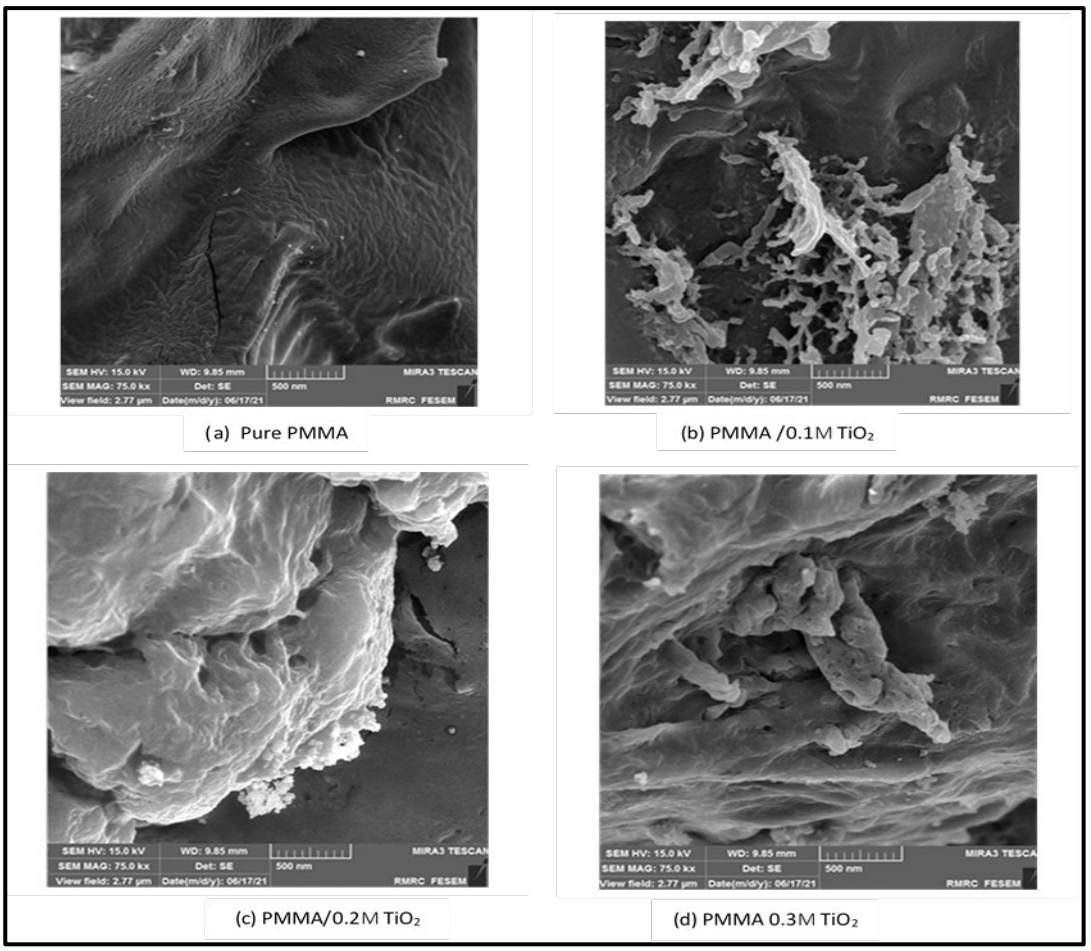

Figure 2 FE-SEM images of pure PMMA and (PMMA/TiO_2) nanocomposite thin films prepared with different TiO_2 concentrations via dip coating at 60 °C.

3.3 Fourier transform infrared (FTIR) analysis

The FTIR spectra provide valuable information about the functional groups in the synthesized materials and confirm the presence of characteristic groups in both pure PMMA and (PMMA/TiO_2) composites. The spectra exhibit a broad absorption band at approximately 3500 cm^{-1}, corresponding to O–H stretching vibrations. This may indicate the interaction of hydroxyl groups with the TiO_2 nanoparticle surface or hydrogen bonding with the PMMA matrix, which is attributed to the use of liquid polymer. The peaks observed around 2950 cm^{-1} correspond to C–H stretching of methyl (CH_3) and methylene (CH_2) groups, which are characteristic of the PMMA backbone.

The strong absorption near 1730 cm^{-1} is assigned to the C=O stretching of the ester carbonyl group in PMMA. In the fingerprint region (1500–500 cm^{-1}), several distinct peaks appear: weak-to-medium bands at 1450–1435 cm^{-1} are due to CH_3 and CH_2 bending vibrations, while the peak near 1380 cm^{-1} corresponds to α-methyl group movements. The band between 1150–1190 cm^{-1} is attributed to C–O–C stretching of the ester group, and the band at 961 cm^{-1} arises from aliphatic CH_2 groups. When comparing the spectra of pure PMMA and (PMMA/TiO_2), slight shifts in peak positions and intensity changes are evident, suggesting interactions between TiO_2 nanoparticles and the PMMA matrix—particularly coordination between Ti atoms and the carbonyl groups of PMMA. Furthermore, new broad absorption bands below 800 cm^{-1} are observed, corresponding to Ti–O–Ti and Ti–O stretching vibrations [13,14].

Overall, these findings confirm the successful incorporation of TiO_2 nanoparticles into the PMMA matrix without altering its fundamental polymer structure, as all characteristic PMMA peaks remain visible.

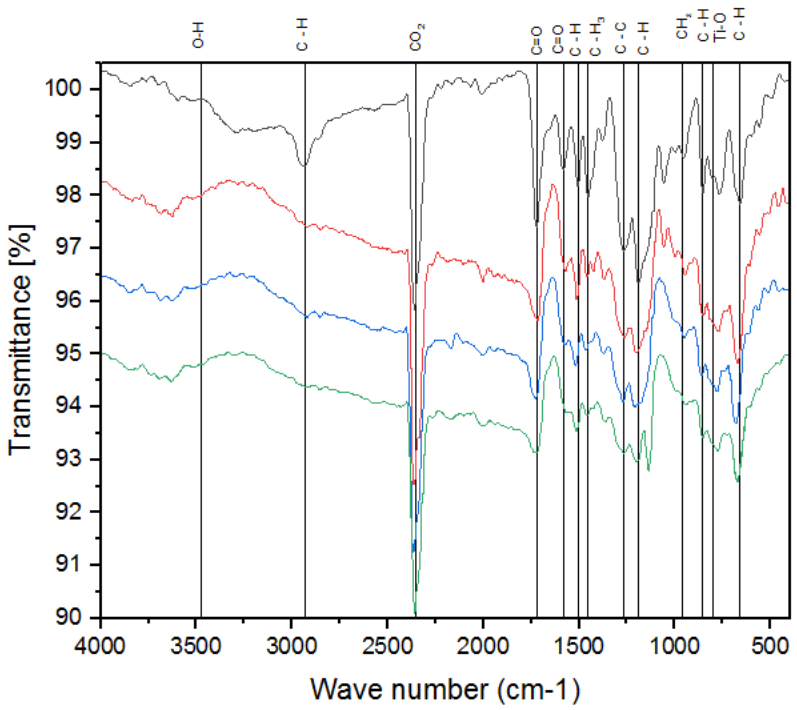

Figure 3 FTIR spectra showing characteristic bonding vibrations of PMMA/TiO_2 nanocomposite thin films.

3.4 Atomic force microscopy (AFM)

Atomic force microscopy (AFM) is used to study the surface topography of the prepared thin films, providing quantitative measurements of grain size, roughness, and surface uniformity, as shown in Table 2 and Figure 4. The 3D AFM images and Gaussian distribution plots indicate that the surface morphology is generally uniform for all samples and most regular in the pure PMMA and 0.1 M TiO_2 films. This can be attributed to the high uniformity of PMMA and the good interaction at low TiO_2 concentration, which enhances film structure and reduces surface roughness.

As the TiO_2 ratio increases, the grain size becomes larger due to structural reorganization and enhanced crystallization within the film, consistent with the XRD results. Conversely, the surface roughness, root mean square (RMS) roughness, and peak-to-peak distance generally decrease with higher TiO_2 content—except for the 0.1 M sample, which exhibits the most significant reduction due to strong TiO_2–PMMA interactions that fill polymer voids and smoothen the surface. In summary, TiO_2 incorporation improves surface distribution, reduces roughness, and promotes the formation of smoother, more uniform thin-film layers.

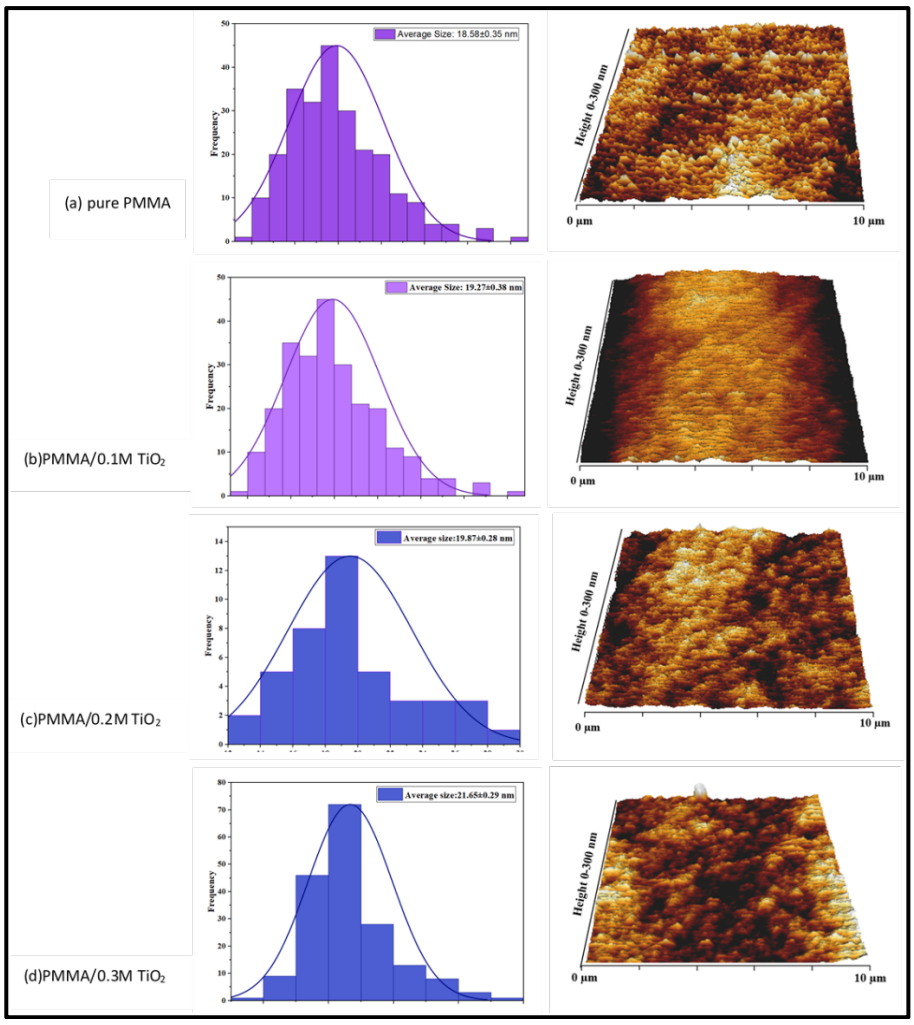

Figure 4 3D AFM images and grain-size distribution of pure PMMA and (PMMA/TiO_2) nanocomposite thin films prepared with different TiO_2 concentrations via dip coating at 60 °C.

Table 2 Effect of TiO_2 concentration on the surface characteristics of the thin films.

Sample	Average Diameter (nm)	Roughness Ave. (pm)	RMS roughness (pm)	Peak-Peak (pm)
PMMA	18.58	168.0	208.9	983.7
PMMA/0.1M TiO_2	19.27	119.2	149.2	583.1
PMMA/0.2M TiO_2	19.87	162.3	194.2	886.8
PMMA/0.3M TiO_2	21.65	158.1	190.3	721.0

4. CONCLUSIONS

The study confirmed that the dispersion of TiO_2 nanoparticles within the PMMA matrix using the dip-coating technique at 60 °C significantly enhanced the structural, morphological, and surface topography properties of the resulting thin films. XRD analysis revealed a transformation from an amorphous to a partially crystalline structure, with the crystallite size increasing from 14 nm to 15 nm as the TiO_2 concentration increased from 0.2 M to 0.3 M. FE-SEM and AFM analyses further

demonstrated a general improvement in film quality, evidenced by an increase in the average grain size from 18.58 nm to 21.65 nm and a reduction in surface roughness from 168.0 pm to 158.1 pm, indicating improved structural uniformity and homogeneity.

References

[1] W.D. Nix, Metall. Trans. A 20 (1989) 2217 https://doi.org/10.1007/BF02666659
[2] H. Geistlinger, Sens. Actuators B: Chem. 17 (1993) 47 https://doi.org/10.1016/0925-4005(93)85183-B
[3] N. Ben Azaza et al., Opt. Mater., 96 (2019) 109328 https://doi.org/10.1016/j.optmat.2019.109328.
[4] I. Armentano, D. Puglia, F. Luzi, C.R. Arciola, F. Morena, S. Martino, L. Torre, Materials 11 (2018) 795 https://doi.org/10.3390/ma11050795
[5] M. M. Abbas, M. Rasheed, J. Phys. Conf. Ser., 1795(1) (2021) 012059 https://doi.org/10.1088/1742-6596/1795/1/012059
[6] M. Rasheed, SuhaShihab, O. Alabdali, H. H. Hassan, J. Phys. Conf. Ser. 1879 (2021) 032113 https://doi.org/10.1088/1742-6596/1879/3/032113
[7] B. A. Sabri, M. Satgunam, N.M. Abreeza, A.N. Abed, Cogent Eng. 8 (2021) 1875968 https://doi.org/10.3390/polym13183083
[8] M. Skocaj, M. Filipic, J. Petkovic, S. Novak, Radiol. Oncol. 45 (2011) 227 https://doi.org/10.2478/v10019-011-0037-0
[9] A.F. Diaz, J. Bargon, Handbook of Conducting Polymers, vol. 1, Marcel Dekker, New York, 1986, p. 81. https://doi.org/10.1007/BFb0025905
[10] Rida Ahmed Ammar, Experimental and Theoretical NANOTECHNOLOGY 2 (2018) 1 https://doi.org/10.56053/2.1.1.
[11] M. Mourad Mabrook, Experimental and Theoretical NANOTECHNOLOGY 2 (2018) 103 https://doi.org/10.56053/2.2.103
[12] A.M. Rheima, M.A. Mohammed, S.H. Jaber, S.A. Hameed, Desalination Water Treat. 194 (2020) 187 https://doi.org/10.1007/BFb0025905
[13] F. M. Shamsudin, S. Radiman, Y. Abdullah, N. A. Hamid, Experimental and Theoretical NANOTECHNOLOGY 3 (2019) 27 https://doi.org/10.56053/3.1.27
[14] A. León, P. Reuquen, C. Garín, R. Segura, P. Vargas, P. Zapata, P.A. Orihuela, Appl. Sci. 7 (2017) 49 https://doi.org/10.3390/app7010049